

3-24-2017

Nutrient and Phytoplankton Dynamics on the Inner Shelf of the Eastern Bering Sea

Calvin W. Mordy
University of Washington

Allan H. (Allan Houston) Devol
University of Washington

Lisa B. Eisner
Alaska Fisheries Science Center (U.S.)

Nancy Kachel
University of Washington

Carol A. Ladd
University of Washington

See next page for additional authors

Follow this and additional works at: https://cedar.wvu.edu/esci_facpubs

Part of the [Environmental Sciences Commons](#), [Marine Biology Commons](#), and the [Oceanography Commons](#)

Recommended Citation

Mordy, C. W., et al. (2017), Nutrient and phytoplankton dynamics on the inner shelf of the eastern Bering Sea, *J. Geophys. Res. Oceans*, 122, 2422–2440, doi:10.1002/2016JC012071.

This Article is brought to you for free and open access by the Environmental Sciences at Western CEDAR. It has been accepted for inclusion in Environmental Sciences Faculty and Staff Publications by an authorized administrator of Western CEDAR. For more information, please contact westerncedar@wwu.edu.

Authors

Calvin W. Mordy, Allan H. (Allan Houston) Devol, Lisa B. Eisner, Nancy Kachel, Carol A. Ladd, Michael W. Lomas, Peter Proctor, Raymond Nicholas Sambrotto, David Shull, Phyllis Jean Stabeno, and Eric Wisegarver

RESEARCH ARTICLE

10.1002/2016JC012071

Nutrient and phytoplankton dynamics on the inner shelf of the eastern Bering Sea

Key Points:

- The inner shelf of the Bering Sea is primarily a regenerative system even in spring
- Sediments are not a significant source of inorganic nitrogen
- Chlorophyll *a* on the inner shelf correlates with wind mixing and the nutrient content on the middle shelf

Supporting Information:

- Supporting Information S1
- Table S1

Correspondence to:

C. W. Mordy,
mordy@uw.edu,
calvin.w.mordy@noaa.gov

Citation:

Mordy, C. W., et al. (2017), Nutrient and phytoplankton dynamics on the inner shelf of the eastern Bering Sea, *J. Geophys. Res. Oceans*, 122, 2422–2440, doi:10.1002/2016JC012071.

Received 17 JUN 2016

Accepted 19 FEB 2017

Accepted article online 23 FEB 2017

Published online 24 MAR 2017

Calvin W. Mordy^{1,2} , Allan Devol³ , Lisa B. Eisner⁴, Nancy Kachel^{1,2}, Carol Ladd² , Michael W. Lomas⁵ , Peter Proctor^{1,2}, Raymond N. Sambrotto⁶ , David H. Shull⁷, Phyllis J. Stabeno² , and Eric Wisegarver²

¹Joint Institute for the Study of the Atmosphere and Ocean, University of Washington, Seattle, Washington, USA, ²Pacific Marine Environmental Laboratory, NOAA, Seattle, Washington, USA, ³School of Oceanography, University of Washington, Seattle, Washington, USA, ⁴Alaska Fisheries Science Center, Seattle, Washington, USA, ⁵Bigelow Laboratory for Ocean Sciences, East Boothbay, Maine, USA, ⁶Lamont-Doherty Earth Observatory, Columbia University Earth Institute, Palisades, New York, USA, ⁷Department of Environmental Sciences, Western Washington University, Bellingham, Washington, USA

Abstract In the Bering Sea, the nitrogen cycle near Nunivak Island is complicated due to limited nutrient replenishment across this broad shelf, and substantial nitrogen loss through sedimentary processes. While diffusion at the inner front may periodically support new production, the inner shelf in this region is generally described as a regenerative system. This study combines hydrographic surveys with measurements of nitrogen assimilation and benthic fluxes to examine nitrogen cycling on the inner shelf, and connectivity between the middle and inner shelves of the southern and central Bering Sea. Results establish the inner shelf as primarily a regenerative system even in spring, although new production can occur at the inner front. Results also identify key processes that influence nutrient supply to the inner shelf and reveal coupling between the middle shelf nutrient pool and production on the inner shelf.

1. Introduction

The most notable topographical feature of the eastern Bering Sea is a broad shelf that extends >500 km offshore [Stabeno *et al.*, 1999]. It is oceanographically partitioned into distinct cross-shelf domains: the coastal (<50 m water depth), middle (50–100 m), and outer shelf (100–200 m) domains [Kinder and Schumacher, 1981a, 1981b; Coachman, 1986]. Waters that occupy these domains are derived from two primary sources; the nutrient-rich Bering Sea basin, and the fresher, nutrient-poor Gulf of Alaska shelf. The Aleutian North Slope Current (ANSC) carries basin water northeastward along the northern slope of the Aleutian Island archipelago, and upon reaching the southeast corner of the Bering Sea basin, the flow turns to the northwest to form the Bering Slope Current (BSC). A portion of the ANSC flows into Bering Canyon supplying Bering Sea basin water to the shelf (Figure 1) [Stabeno *et al.*, 2016]. North of Unimak Pass, Bering Sea basin water is joined by Gulf of Alaska shelf water (via the Alaska Coastal Current that flows north through Unimak Pass), and it is this mixture of basin and shelf waters that serves as the origin of water that covers most of the inner shelf (Figure 1) [Stabeno *et al.*, 2016].

Downstream of Bering Canyon, flow over the inner shelf continues to the northeast supplying nutrients along the Alaskan peninsula and into Bristol Bay. In Bristol Bay, the flow turns to the northwest toward Nunivak Island. Because this flow is sluggish ($\sim 2 \text{ cm s}^{-1}$), the transit time from Bering Canyon to Nunivak Island is ~ 1 year [Stabeno *et al.*, 2016]. During this lengthy transit, waters over the inner shelf are modified by ice formation and melt, runoff, primary production, nutrient drawdown and remineralization, and sedimentary processes, and it is this modified water near Nunivak Island (Region 7 in Figure 1) that serves as the focus of this study.

In winter, the water column over the middle and inner shelf is usually well mixed [Stabeno *et al.*, 2001]. In spring, a two-layer system develops over the middle domain while the inner shelf remains vertically mixed due to a combination of tidal and wind mixing [Schumacher *et al.*, 1979; Kachel *et al.*, 2002]. The inner front, which separates these two regimes, is distinct from Unimak Pass to north of Nunivak Island, and is nominally located along the 50 m isobath, although it can vary depending on the strength of wind and tidal mixing [Schumacher *et al.*, 1979; Schumacher and Stabeno, 1998; Overland *et al.*, 1999; Stabeno *et al.*, 2001; Kachel *et al.*, 2002]. In

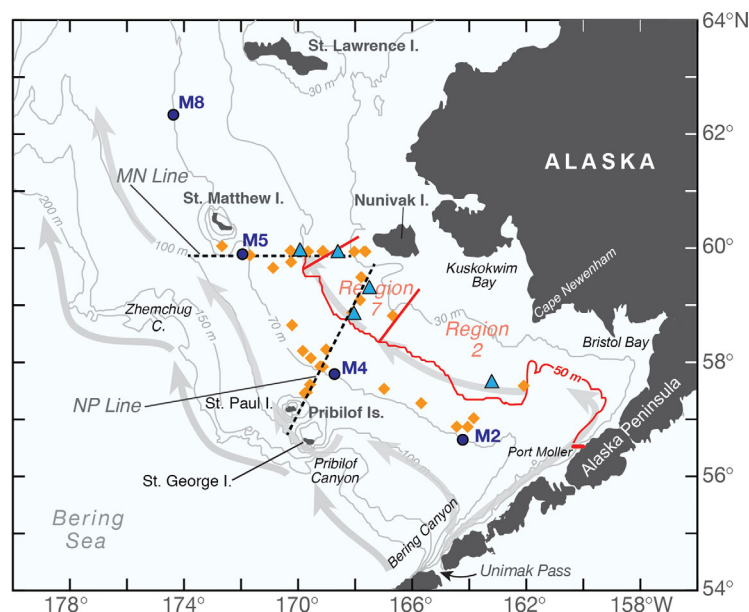


Figure 1. Map of the eastern Bering Sea showing a generalized pattern of flow [Stabeno *et al.*, 2016] and inner shelf Regions 2 and 7 as defined by Ortiz *et al.* [2012]. Also shown are the locations of long-term moorings M2, M4, M5, and M8 (blue dots); the MN and NP hydrographic lines (dashed lines); assimilation stations (orange diamonds); and benthic sampling stations (blue triangles).

summer, mixing at the inner front can erode into the bottom layer of the middle shelf and introduce nutrients into the upper water column [Stockwell *et al.*, 2001; Kachel *et al.*, 2002], and this in turn supports primary and secondary production [Sambrotto *et al.*, 1986; Whitedge *et al.*, 1986; Stockwell *et al.*, 2001; Coyle and Pinchuk, 2002; Kachel *et al.*, 2002; Rho and Whitedge, 2007; Coyle *et al.*, 2011; Zador, 2013]. The effectiveness of nutrient pumping at the front (i.e., the diffusive nutrient flux), however, varies on tidal to annual scales and depends on the availability of nutrients in the bottom layer of the middle shelf adjacent to the front [Stockwell *et al.*, 2001; Kachel *et al.*, 2002].

The nutrient content on the middle shelf, and hence the potential for nutrient pumping at the inner front, is governed in large part by winter replenishment from the slope. On the middle shelf, Stabeno *et al.* [2016] found that during late fall and winter, on average $\sim 50\%$ of middle shelf water is replaced by water from the slope and Unimak Pass, but there was substantial interannual variability in the extent of wintertime replenishment. On the inner shelf near Nunivak Island, replenishment is more limited. Isotopic evidence suggests that nitrate is largely the result of local nitrification with little evidence of slope water reaching this far inshore [Granger *et al.*, 2013]. Compounding the low rates of nitrogen replenishment on the inner shelf is the loss of inorganic nitrogen through denitrification and/or anaerobic ammonium oxidation (anammox), i.e., microbial production of nitrogen gas [Horak *et al.*, 2013]. As a result, portions of the inner shelf may have chronically low concentrations of nitrate for much of the year.

The seasonal cycle of nitrate at the 50 m isobath was originally established in 1979–1981 off Cape Newenham with concentrations declining each year from $\sim 10 \mu\text{M}$ in May to $< 1 \mu\text{M}$ in June, and a modest increase in nitrate during late summer and fall [Whitedge *et al.*, 1986]. In 1997–1999, observations across the middle and inner shelves in May and August found that nitrate decreased from the middle to the inner shelf, and the inner shelf was generally depleted in nitrate at Port Moller, Cape Newenham, and Nunivak Island [Kachel *et al.*, 2002]. It was unclear if nitrate depletion reflected postbloom conditions, or if nitrate was chronically low. Strong gradients in nitrate across the shelf imply a shift from new production on the middle shelf (i.e., primarily nitrate assimilation) to regenerated production on the inner shelf (i.e., primarily ammonium assimilation).

In the vicinity of Nunivak Island (Region 7, Figure 1), spring conditions on the inner shelf may differ from those near Cape Newenham and along the Alaskan Peninsula. Region 7 is usually ice covered, and these waters have likely been modified by the annual production cycle during the ~ 1 year transit from Bering Canyon [Stabeno *et al.*, 2016]. In summer, the advective nutrient flux into this region is presumed to be small due to weak currents and low concentrations upstream of Nunivak, so other sources of nutrients are likely supporting primary production. For example, in September 1997, Stockwell *et al.* [2001] observed moderate concentrations of nitrate ($\sim 1 \mu\text{M}$) and chlorophyll *a* ($\sim 3 \mu\text{g L}^{-1}$) inshore on the NP Line, and attributed this to nitrification.

In this study, two sets of questions will be addressed that are critical for understanding the nitrogen cycle in Region 7 of the inner shelf. The first set relates to the distribution and uptake of nutrients including: what are nutrient levels in spring that support production; what is the timing of spring production and rates of production and nutrient drawdown in these relatively shallow, ice-covered waters; and how do

new and regenerated production vary across the shelf in spring and summer? To address this set of questions, we compiled spring and summer data collected in 2007–2010 as part of the Bering Sea Project (<http://www.nprb.org/bering-sea-project>), a multidisciplinary investigation of the regional ecosystem. These data are used to examine the seasonal distribution of nutrients in the region, and evaluate assimilation rates of carbon, nitrate, and ammonium across the shelf in spring and summer.

The second set of questions relates to the source of nutrients in summer: what are the sources of nutrients that sustain postbloom production; and how does postbloom production at the inner front vary with the diffusive flux? To address these questions, we estimate the benthic efflux of dissolved inorganic nitrogen (DIN = nitrate + nitrite + ammonium) using benthic rate measurements determined during the Bering Sea Project, estimate nitrogen input from the Kuskokwim River, and estimate rates of nitrification. To examine variability in the diffusive nutrient flux, we use data from the Bering Sea Project, as well as a chlorophyll time series that began in 2003 as part of NOAA's Bering Arctic Subarctic Integrated Survey (BASIS). The BASIS chlorophyll data are related to an index of wind mixing, and an estimate of replenishment of bottom waters on the middle shelf.

2. Methods

Data from the Bering Sea Project were collected during hydrographic cruises between 2007 and 2010 that spanned the inner front with spring cruises in 2007–2009, and summer cruises in 2008–2010 (Table 1). Measurements taken include temperature, salinity, oxygen, chlorophyll *a*, nutrients, rates of nitrogen and carbon assimilation, rates of sedimentary denitrification/anammox, oxygen consumption, and efflux of nitrogen (nitrate, nitrite, ammonium), but not all measurements were made in each year, in each season, or at each station. Analytical methods for these measurements are described in sections 2.1–2.3.

The BASIS survey collected hydrographic data along a 0.5° latitude × 1° longitude survey grid that spans the shelf with stations spaced ~60 km apart [Eisner *et al.*, 2016]. Stations on the inner shelf south of 60°N (Regions 7 and 2, see Figure 1) were occupied between late August and mid-September. Integrated chlorophyll is the sole data set presented from BASIS, and sampling and measurement techniques were comparable to methods described below for the Bering Sea Project.

2.1. Hydrographic Sampling and Analysis

Conductivity-temperature-depth (CTD) measurements were made using a Seabird SBE 911plus system with dual temperature, conductivity (salinity), and oxygen (SBE-43) sensors, and single sensors for Photosynthetically Active Radiation (PAR, Biospherical Instruments QSP-200 L4S, QSP-2300, or QSP2000) and chlorophyll *a* fluorescence (WET Labs WETStar WS3S). Data were recorded during the downcast, with a descent rate of 15 m min⁻¹ to a depth of 35 m, and 30 m min⁻¹ below that. Temperature probes were calibrated by the manufacturer, and the primary and secondary probes generally agreed to within 0.002°C. Salinity calibration samples were taken on alternate casts and analyzed on a laboratory salinometer. These calibrations indicate instrument accuracy better than 0.01. The oxygen sensors were calibrated from Winkler analysis of discrete samples collected at one or more depths on each cast. Chlorophyll *a* fluorescence was converted into concentration using discrete samples filtered on GF/F filters, and analyzed using the traditional acidification fluorescence method of *Strickland and Parsons* [1972].

Samples for dissolved nutrient analysis (nitrate, nitrite, ammonium, phosphate, and silicic acid) were syringe-filtered using 0.45 μm cellulose acetate membranes and collected in 30 mL acid-washed, high-density polyethylene bottles after three rinses. Samples were analyzed shipboard within 1–12 h of collection. Nutrients

were determined using a combination of analytical components from Alpkem, Perstorp, and Technicon. We closely followed the WOCE-JGOFS standardization and analysis procedures specified by *Gordon et al.* [1993], including reagent preparation, calibration of labware, preparation of primary and secondary standards, and corrections for blanks and

Table 1. Hydrographic Cruises During the Bering Sea Project

Year	Season	Vessel	Cruise ID	Cruise Dates
2007	Spring	Healy	HLY-07-01	4/10 to 5/12
2008	Spring	Healy	HLY-08-02	3/31 to 5/6
	Summer	Healy	HLY-08-03	7/3 to 7/31
2009	Spring	Healy	HLY-09-02	4/3 to 5/12
	Summer	Knorr	KN-195-10	6/14 to 7/13
2010	Early summer	Thompson	TN-249	5/9 to 6/14
	Summer	Thompson	TN-250	6/16 to 7/13

refractive index. Ammonium was measured using an indophenol blue method modified from *Mantoura and Woodward* [1983].

2.2. Assimilation of Carbon and Nitrogen

Methods for determination of nitrate and ammonium uptake rates using ^{15}N , and primary productivity using ^{13}C and ^{14}C were detailed by *Sambrotto et al.* [2016] and *Lomas et al.* [2012]. The two referenced methods were identical in sampling depths and on-deck incubations. Daily simulated in situ productivity incubations were conducted on deck with incubation bottles screened to 100, 55, 30, 17, 9, 5, and 1.5% of surface light levels; the light levels at each depth from which samples were originally collected. Incubations were conducted for a full 24 h for ^{14}C . This also was the incubation period for most of the combined ^{15}N and ^{13}C tracer experiments that were done in a single incubation bottle. Shorter (~ 6 h), dual ^{15}N and ^{13}C incubations were done in situ by suspending bottles through a hole in the ice at their original sample depth. Estimates of daily rates were extrapolated from the in situ rates by assuming a 12 h production period.

The amount of the ^{15}N tracer added was based on the preliminary measurement of their respective pool sizes to achieve a nitrogen tracer concentration equal to about 10% of the initial pool. Stable isotopic ratios of N and C and total nitrogen and carbon content in the postincubation filtered particles were measured with a Europa 20-20 mass spectrometer in continuous flow mode using an automated ANCA combustion system. Uptake rates were calculated from the equations in *Dugdale and Goering* [1967].

Rates of net primary production (NPP) were calculated from the autotrophic incorporation of $\text{NaH}^{14}\text{CO}_3^-$ into particulate organic matter (i.e., particles $\geq 0.7 \mu\text{m}$; Ahlstrom 151 filters) using the ratio of added radio-carbon, $\sim 10 \mu\text{Ci}$ of $\text{NaH}^{14}\text{CO}_3^-$, to total inorganic carbon present (based upon salinity) [*Lomas et al.*, 2012]. Following filtration, samples were rinsed with 10% HCl to remove residual $\text{NaH}^{14}\text{CO}_3^-$ and counted on a Perkin Elmer TriCarb 2900LR after the addition of 5 mL of Ultima Gold (Perkin Elmer, USA) scintillation cocktail. Daily volumetric rates of NPP were calculated from the mean light bottle value corrected for the dark bottle value using the average total added activity for the profile [*Lomas et al.*, 2012].

2.3. Sediment Denitrification, Respiration, and Nitrogen Efflux

Rates of sediment respiration and denitrification/anammox were determined by incubating intact sediment cores at in situ temperatures and measuring the change in concentration of nutrients, dissolved oxygen and dissolved nitrogen gas in the overlying water. Sediment cores were collected with an Ocean Instruments MC 800 multicorer, which can collect up to eight undisturbed 10 cm diameter cores up to 40 cm in length. Bottom water was collected at each station using a Niskin bottle attached to the multicorer. These cores were subcored using 8 cm diameter polyethylene terephthalate tubes that held ~ 20 cm segment with ~ 10 cm of head space. At each station, two or three replicate cores (depending on coring success) were sealed with silicone stoppers and connected to a reservoir containing bottom water as described by *Davenport et al.* [2012]. These flux cores were sampled for nutrients and dissolved gases over a period of 3–5 days, depending on the reaction time.

Oxygen concentration in the overlying water of the incubation cores was measured using a PreSens Microx TX3 fiber optic oxygen meter with a needle-type PreSens optode from 5 mL subsamples. The optode was calibrated using air equilibrated seawater and seawater deoxygenated with sodium sulfite. The initial change in oxygen concentration during the incubation period was determined by one of two methods: (1) fit a polynomial to all the data and determine the derivative of that polynomial function at $t = 0$; (2) if the data did not fit a polynomial well, the flux at $t = 0$ was calculated from the linear slope of the first two points. Oxygen fluxes were corrected to account for the addition of reservoir water to the core incubation and the slow desorption of oxygen from the silicone caps of the incubation cores [*Davenport et al.*, 2012].

To determine rates of sedimentary denitrification/anammox, we measured dissolved nitrogen/argon ratios in the overlying water of each flux core using a membrane inlet mass spectrometer [*Kana et al.*, 1994; *Chang and Devol*, 2009]. The incubation was terminated when the O_2 concentration dropped below 50% of the initial concentration. At HLY0902, Station 9, a mass balance approach was used to estimate the denitrification rate [*Horak et al.*, 2013]. This assumes that the denitrification rate is the difference between NH_4^+ produced from sedimentary aerobic respiration and the net DIN flux out of the sediment.

2.4. Reanalysis Winds and Sea Ice

An index of wind mixing was determined around the M2 and M4 moorings using data from the National Center for Environmental Prediction (NCEP), Department of Energy Reanalysis. NCEP uses a state-of-the-art analysis/forecast system to perform data assimilation on a 2.5° latitude by 2.5° longitude grid with data ranging from January 1979 to present [Kalnay et al., 1996; Kanamitsu et al., 2002]. NCEP winds are well correlated with the observed winds in the Bering Sea [Ladd and Bond, 2002]. Reanalysis data were obtained from the NOAA Earth System Research Laboratory, Physical Sciences Division in Boulder, Colorado, USA, from their website at <http://www.esrl.noaa.gov/psd/>. At each mooring location, the daily values of the winds were averaged in a 2° latitude \times 5° longitude box centered on the moorings. The wind mixing index is based on the friction velocity (u_*^3) deduced from daily values of the surface stress/momentum flux (N. Bond, University of Washington, Seattle).

Sea ice extent and areal concentration was provided by the Advanced Microwave Scanning Radiometer EOS, which consists of daily ice concentration data at 12.5 km resolution, and are available from the National Snow and Ice Data Center (NSIDC) website.

2.5. Location of the Inner Front

The location and width of the inner front across the shelf was determined from the changes in the vertical structure of the thermocline ($|dT/dz|$, where z is the vertical component and T is temperature). Kachel et al. [2002] defined the offshore extent of the inner front as the location where the temperature gradient declines by 50%, or $|dT/dz| < 0.5 |dT/dz|_{\max}$ where $|dT/dz|_{\max}$ is the absolute maximum value along the cross-front transect. The inshore extent was defined as the location where $|dT/dz| < 0.05^\circ\text{C m}^{-1}$.

3. Results

Results from the Bering Sea Project are presented including oceanographic conditions across the shelf, assimilation across the middle and inner shelves, and benthic oxidation and denitrification/anammox on the inner shelf. Oceanographic conditions are described through a series of hydrographic sections in 2009 (supporting information figures include sections from 2008 and 2010), mapping the location of the inner front on surface maps of physical and chemical properties, and the seasonal distribution of nutrients on the inner shelf. BASIS data are presented in the discussion during an examination of the diffusive nutrient flux. Mean values are given as the mean \pm SE (N), except when noted as SD.

3.1. Hydrography of the Middle and Inner Shelves

During the Bering Sea Project, a series of hydrographic transects were occupied in spring and summer that crossed the middle shelf and converged in Region 7 (as defined by Ortiz et al. [2012]). The MN Line extends from Nunivak Island toward St. Matthew Island, and the NP Line extends from Nunivak Island toward the Pribilof Islands (Figure 1). The NP Line crosses the central middle shelf near the M4 long-term mooring while the MN Line lies in the transition zone between the northern and southern shelves, and crosses the M5 long-term mooring.

In spring of each year (2007–2009), the distributions of properties across the middle and inner shelves were similar, so only sections from the 2009 MN Line are shown (Figure 2). During our field years (2007–2010), cold conditions prevailed in the Bering Sea with maximum ice extent usually as far south as $\sim 56^\circ\text{N}$, and occurring between 22 March (2007) and 3 April (2010) [Stabeno et al., 2012b]. Hence, during our spring surveys, the MN and NP lines were mostly covered by sea ice, although in 2007, Region 7 was sampled later in spring when ice retreat had commenced. The MN and NP lines were characterized by a weakly stratified or well-mixed water column with temperatures typically -1.7°C . Salinity and concentrations of nitrate and silicic acid decreased from the outer shelf to the coastal domain: the middle shelf had relatively high concentrations of nitrate, ammonium and silicic acid, and low concentrations of chlorophyll *a* while the inner shelf was nutrient-poor despite impedance of light due to spring sea-ice cover.

In summer, a two-layer system develops over the southern middle shelf, with a strong pycnocline separating a 20–30 m wind-mixed surface layer (fresher, warmer, and nutrient poor) from a tidally mixed, nutrient replete bottom layer [Stabeno et al., 2012a]. In 2008 (supporting information Figures S1 and S2) and 2009 (Figures 3 and 4), the stratified two-layer structure extended shoreward to ~ 50 m isobath. Over the inner shelf, the water column was well mixed or weakly stratified; and relative to bottom waters of the middle shelf, the inner shelf was fresher, warmer, and nutrient poor. Most notably, in summer 2008 and 2009, there was little DIN on the inner shelf. Nitrate concentrations were near the detection limit ($0.08 \mu\text{M}$), and ammonium was typically < 0.5

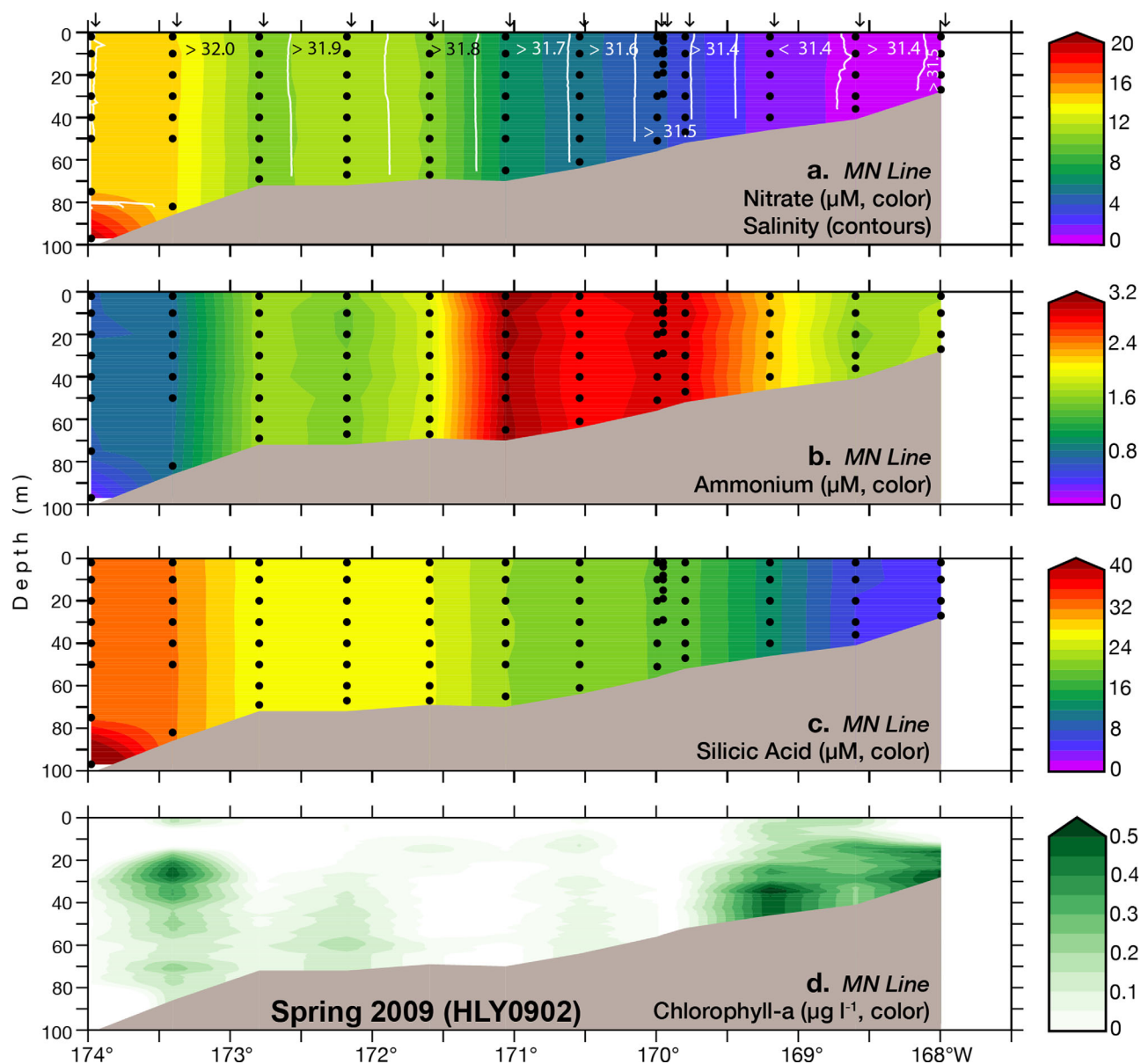


Figure 2. Hydrographic sections along the MN Line during 6–9 April 2009 of (a) nitrate (color) and salinity (contours, 0.1 interval), (b) ammonium, (c) silicic acid, and (d) chlorophyll *a*.

μM . Despite the paucity of reactive nitrogen, appreciable concentrations of chlorophyll *a* ($10\text{--}15 \mu\text{g L}^{-1}$) were observed at the inner front along the MN Line in summer 2009, and associated with this feature was a surface expression of silicic acid ($9.4 \mu\text{M}$) that was not evident in nitrate or ammonium (Figure 3). This result is consistent with a diffusive flux of nutrients at the inner front and consumption of nitrogen by a phytoplankton community largely devoid of diatoms, resulting in a residual pool silicic acid. These features were not observed along the inner front of the NP Line in summer 2009 (Figure 4). (Near the outer shelf of the NP Line, the water column shoals and is fully mixed in the vicinity of the Pribilof Islands ($\sim 170^\circ\text{W}$) with enhanced chlorophyll concentrations and associated nutrient drawdown (Figure 4). These features around the Pribilof Islands have been addressed elsewhere [Sullivan *et al.*, 2008; Stabeno *et al.*, 2008] and will not be discussed here.)

In summer 2008, there was a small surface expression of silicic acid ($2.3 \mu\text{M}$) at the inner front along the NP Line concomitant with a relatively small chlorophyll maximum ($\sim 1.5 \mu\text{g L}^{-1}$) (supporting information Figure S2), but similar features were not observed along the MN Line (supporting information Figure S1). In summer 2010, stratification along the MN Line extended to the inshore station due to a pool of warm, low-salinity water that resulted from late ice retreat, and this stratified water disrupted the inner front (supporting information Figure

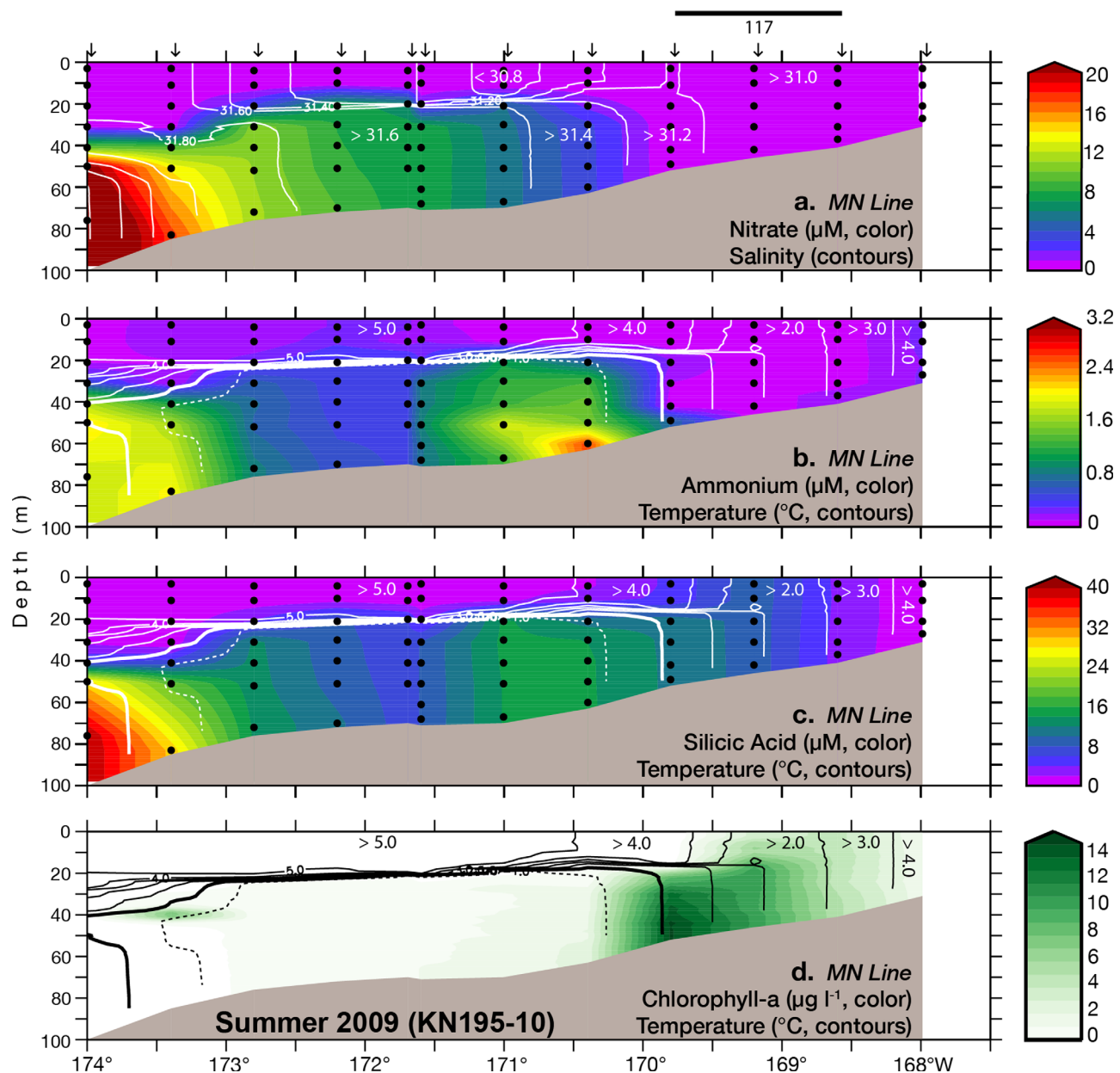


Figure 3. Hydrographic sections along the MN Line during 1–2 July 2009 of (a) nitrate (color) and salinity (contours, 0.2 interval), (b) ammonium and temperature (1° interval), (c) silicic acid and temperature, and (d) chlorophyll *a* and temperature. The thicker temperature contour line is 0°C , and the dashed line is -1°C . The bar on top of the figure indicates the location of the inner front. The location of Cast 117 is also noted. Note a different scale for chlorophyll *a* than in Figure 2.

S3). Nevertheless, moderate levels of ammonium and chlorophyll were observed in the bottom layer of the inner shelf. Together, results from these summertime hydrographic sections reveal the spatiotemporal variability in the diffusive flux of nutrients at the inner front, as defined through patterns of stratification and silicic acid, and these spatial patterns are further examined in the ensuing surface maps from summer 2009.

The inner front in summer 2009 was plotted on maps of near-surface (<8 m) temperature, salinity, and silicic acid (Figure 5). Along the MN Line ($\sim 60^{\circ}\text{N}$), temperatures in the inner front were cooler, and there was a surface expression of silicic acid (as shown in Figure 3). South of the MN Line, the seaward edge of the inner front followed the 50 m isobath southeast toward Bristol Bay, and cooler surface water was associated with the inner front. However, south of the MN Line, surface concentrations of silicic acid in the inner front remained low. North of the MN Line, a band of warmer and fresher water extended inshore from the 50 m isobath. This water was stratified (not shown), and directed the inner front to the northeast. North of 61°N ,

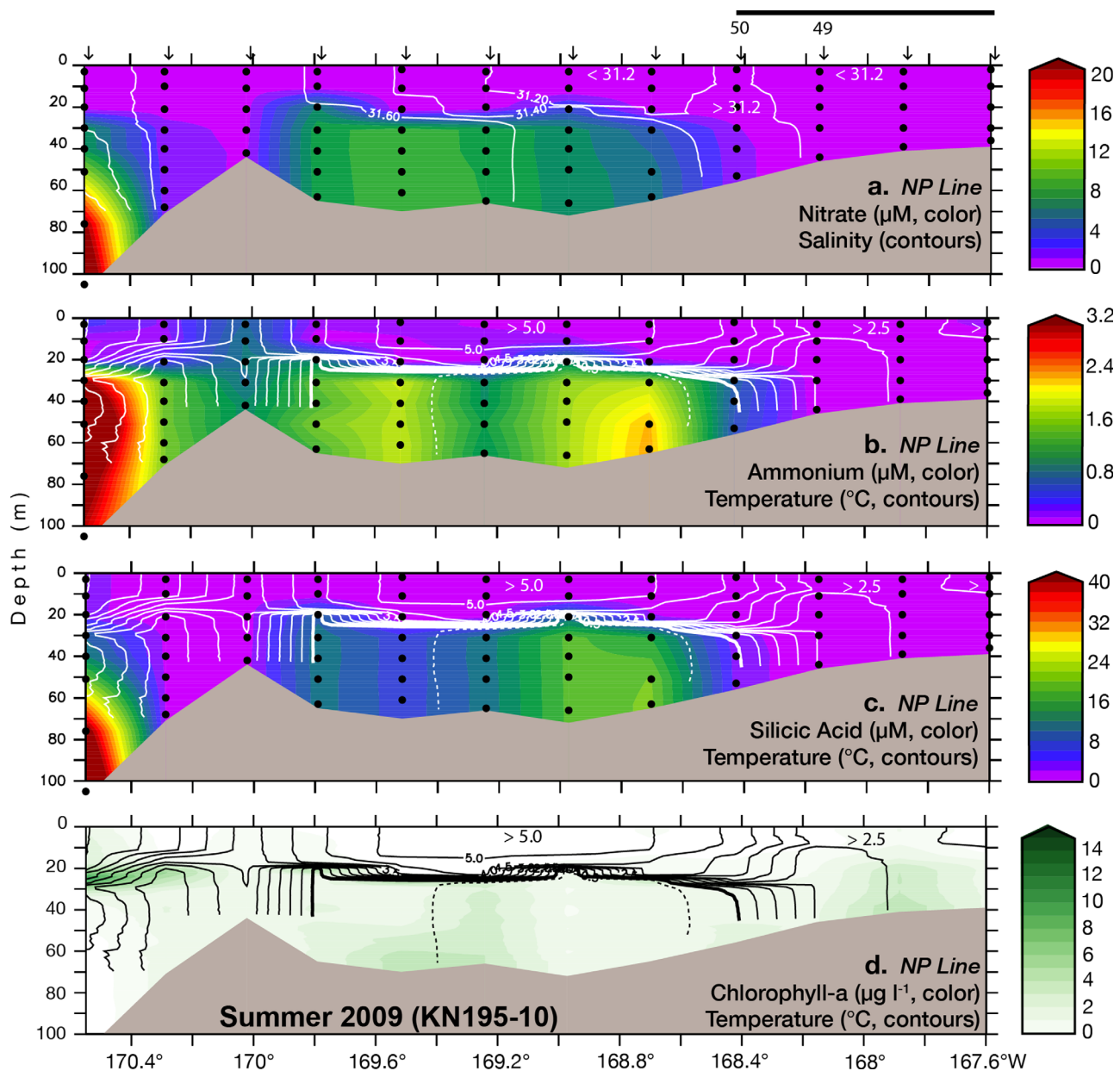


Figure 4. Hydrographic sections along the NP Line during 22–23 June 2009 as in Figure 3 except the temperature contour interval is 0.5°C. The location of Casts 49 and 50 are indicated at the top of the figure.

the upper water column was cooler, fresher, and stratified (not shown). Although the inner shelf north of the MN Line was stratified, there was a large pool of silicic acid (Figure 5c). Silicic acid concentrations at the five inner shelf stations within this pool were relatively uniform with depth ($14 \pm 3 \mu\text{M}$ (26), $\pm\text{SD}$).

These results indicate that in summer, a surface expression of silicic acid is not necessarily an indicator of the diffusive flux of nutrients (which was likely absent in stratified waters to the north) nor is the cold band associated with the inner front always coupled with diffusion of nutrients (absence of surface silicic acid to the south). The latter assumes that diatoms were of minor importance in summer [Stoecker *et al.*, 2014], although storm mixing can induce diatom production [Sambrotto *et al.*, 1986].

3.2. Seasonal Distribution of Nutrients and Chlorophyll *a* on the Inner Shelf

To examine the variability of reactive nitrogen and chlorophyll *a* on the inner shelf west and south of Nunivak Island, data from Region 7 in all years were combined (Figure 6). The highest nitrate concentrations (6.8–7.1 μM)

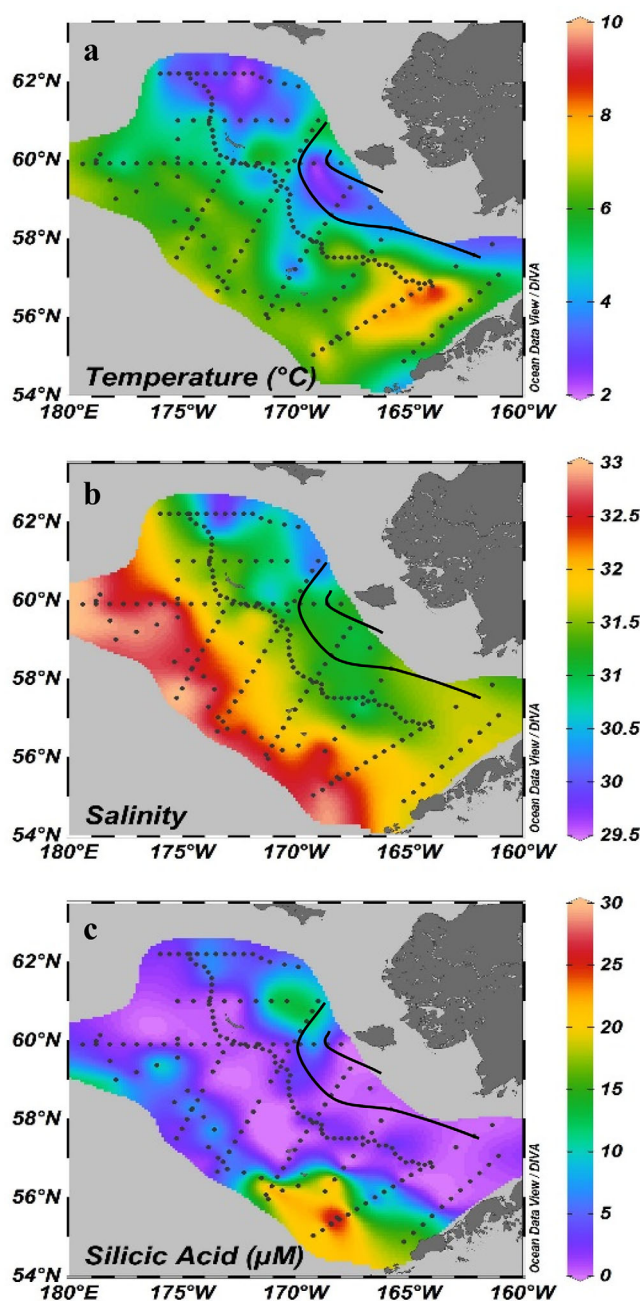


Figure 5. Maps of near-surface (<8 m) temperature ($^{\circ}\text{C}$), salinity and silicic acid (μM) summer 2009 with location of the inner front (black lines) as determined by Kachel *et al.* [2002] and described in section 2.5.

that most of the chlorophyll on the inner shelf in summer was associated with small (<5–10 μm) particles [Lomas *et al.*, 2012; Eisner *et al.*, 2016].

3.3. Assimilation Across the Shelf

To examine trends in assimilation across the inner front, assimilation rates of carbon, nitrate, and ammonium were measured inshore of the 70 m isobath at 27, 10, and 7 stations, respectively, including three stations in <70 m of water between M4 and the Pribilof Islands. These data along with associated water properties appear in supporting information Table S1. While most stations on the inner shelf were from Region 7, the data set includes a sole inner shelf station from Region 2 that was sampled in summer 2009 (KN-195-10, Station 18, supporting information Table S1) as this station provides contrast between new versus

were from a cast near the 50 m isobath in 2007 (45 m bottom depth). This station appeared to be influenced by the deep nutrient pool on the middle shelf, as concentrations were similar to concurrent measurements on the 60 m isobath. Discounting this cast, spring concentrations of nitrate and ammonium were strikingly similar in magnitude, with the highest concentrations (2.1–4.4 μM) observed on the earliest spring cruise (2008) when ice concentrations were $\sim 100\%$. During a later spring cruise in 2007, ice concentrations were highly variable, and nitrate and ammonium concentrations were lower (0.0–1.4 μM).

Assuming this pattern reflects the seasonal drawdown of nutrients, nitrate and ammonium drawdown rates in spring were determined from the regression of vertically integrated data, equaling $2.5 \pm 0.5 \text{ mmol NO}_3 \text{ m}^{-2} \text{ d}^{-1}$ (24) and $3.4 \pm 0.7 \text{ mmol NH}_4 \text{ m}^{-2} \text{ d}^{-1}$ (24), respectively. (Drawdown rates could have been determined from concentration changes between spring and summer cruises; however, blooms on the shelf appeared to occur on much shorter time scales [Sigler *et al.*, 2014].) In summer, although mean nitrate concentrations were near the detection limit ($0.07 \pm 0.01 \mu\text{M}$ (117)), there was measurable ammonium ($0.27 \pm 0.02 \mu\text{M}$ (117)) that may have supported regenerated production (Figures 6a and 6b).

Large accumulations of chlorophyll *a* were not observed during the 2008 and 2009 spring surveys on the inner shelf, but were apparent on the 2007 spring cruise (Figure 6c and Table 2), a pattern also observed for assimilation rates (discussed below). Higher concentrations were also observed during summer, and observations in 2008 and 2009 found

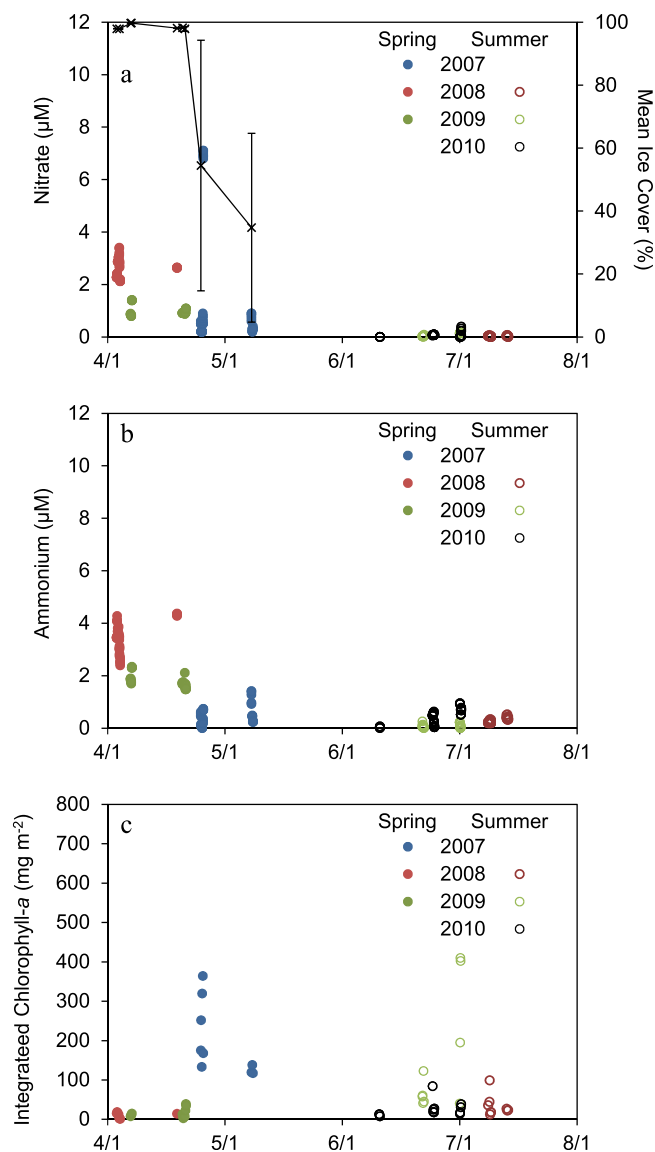


Figure 6. Seasonal distribution of (a) nitrate, (b) ammonium, and (c) integrated chlorophyll *a* (full water column) in Region 7. In Figure 6a, crosses and the black line and error bars (\pm SD) represent mean ice coverage 7 days prior to sampling. For example, on 25 April 2007, six stations were sampled, and the average ice coverage 7 days prior to sampling was determined at each station. These values ranged from 6% to 98%, and the mean of these weekly averages was $55 \pm 40\%$ (\pm SD).

2). The total nitrogen assimilation rates in spring were approximately three times that in summer ($p = 0.04$). For comparing nitrogen assimilation with benthic rates of oxidation, rates of total nitrogen assimilation between April and August was determined by giving equal weight to spring and summer (i.e., ~ 60 days), and taking the mean of these two seasons ($5.8 \pm 5.5 \text{ mmol N m}^{-2} \text{ d}^{-1}$, Table 2).

The *f*-ratio is an estimate of new versus regenerated production and is determined from the ratio of nitrate to total nitrogen uptake (nitrate uptake/nitrate + ammonium uptake) [Dugdale and Goering, 1967]. Only seven measurements of *f*-ratios were available across the middle and inner shelf in this region, and those ratios varied between 0.04 and 0.88 (supporting information Table S1). While there was no significant difference between the *f*-ratios in spring and summer ($p = 0.17$), the lowest *f*-ratios were found in summer. In spring, there was a strong relationship ($R^2 = 0.997$) between the *f*-ratio and mean salinity (Figure 7). The highest ratios were observed in saltier waters near the 70 m isobath where nitrate concentrations were relatively high ($>8 \mu\text{M}$) compared to lower ratios in the coastal domain where nitrate concentrations were $<0.7 \mu\text{M}$

regenerated production in summer. Table 2 summarizes subsets of assimilation data from different regions and periods from supporting information Table S1, and is used to examine prebloom (2008 and 2009) versus bloom (2007) conditions over the middle and inner shelves, and total nitrogen assimilation on the inner shelf in spring, summer, and over the entire measurement period (April–August).

To determine the C:N uptake ratio inshore of the 70 m isobath, simultaneous measurements of carbon, nitrogen, and ammonium uptake were made in spring 2007 ($N = 4$) and summer 2009 ($N = 3$). The ratio of carbon to nitrogen (nitrate + ammonium) uptake averaged 7.9 ± 2.4 (7), and was consistent with the Redfield C:N ratio of 6.625 [Redfield, 1958] supporting the use of Redfield C:N in supporting information Table S1 for converting carbon uptake rates into nitrogen.

In spring, carbon and nitrate uptake rates across the middle and inner shelves were significantly higher in 2007 than in 2008 and 2009 (Table 2). These results were consistent with higher concentrations of chlorophyll *a* in 2007 (Figure 6c and Table 2), and consistent with prebloom sampling in 2008 and 2009 and sampling during the bloom in 2007 as inferred from patterns in the spring nutrient data (Figures 6a and 6b).

Rates of total nitrogen assimilation on the inner shelf in spring and summer were determined by averaging together rates of carbon assimilation (converted into nitrogen units) and nitrogen uptake (simultaneous measurements of nitrate + ammonium) in each season (Table

Table 2. Summarized Values From Supporting Information Table S1 of Integrated Chlorophyll and Assimilation Rates for Different Periods and Regions as Discussed in the Text^a

Period	Region (N)	Z _{eu} Integrated Chlorophyll (mg m ⁻²)	Carbon Assimilation (mmol N m ⁻² d ⁻¹)	Nitrate Assimilation (mmol N m ⁻² d ⁻¹)	Ammonium Assimilation (mmol N m ⁻² d ⁻¹)	Total Nitrogen Assimilation (mmol N m ⁻² d ⁻¹)
Spring 2007	IS (2) and MS (2)	108 ± 21 (4)	13 ± 2 (4)	6 ± 2 (4)		
Spring 2008 and 2009	IS (1) and MS (7)	11 ± 3 (8)	2 ± 1 (8)	0.2 ± 0.1 (2)		
Spring, all years	IS		7 ± 4.2 (4)	2.3 ± 1.5 (3)	8.7 ± 5.3 (2)	8.7 ± 3.0 (6)
Summer, all years	IS		1.9 ± 0.5 (7)	0.5 ± 0.2 (4)	4.5 ± 2.5 (3)	2.9 ± 0.9 (10)
Spring and summer, all years	IS					5.8 ± 5.5

^aNot all measurements were made at each station. Carbon assimilation was converted into nitrogen using the C:N Redfield ratio of 106:16. Total nitrogen assimilation was determined by averaging together carbon assimilation (converted to nitrogen) with nitrate+ammonium assimilation (only when these parameters were measured simultaneously, therefore N values do not sum). Total nitrogen assimilation in spring and summer was determined by assigning an equal weight (60 d) to the mean in each season. Mean values are given as the mean ± SE (N).

(supporting information Table S1). In summer, only three measurements were made, and the *f*-ratio was especially low (≤ 0.05) at two stations having silicic acid concentration $< 1 \mu\text{M}$. But in summer 2009, Station 117 occupied a region of the inner front where mixing appeared to have eroded the deep nutrient pool of the middle shelf, introducing silicic acid (Figure 3) and presumably nitrate into the upper water column. The *f*-ratio of 0.5 at this station was consistent with spring assimilation rates for that salinity (Figure 7).

3.4. Benthic Oxygen Demand and Production of Nitrogen Gas (N₂) on the Inner Shelf

Flux cores on the inner shelf south of 60°N were used to determine: (a) the benthic oxygen demand (BOD), which provides a measure of remineralization of organic material; (b) the rate of N₂ production from denitrification and/or anammox (Table 3). As only five cores were collected in this domain, the data are too sparse to examine spatiotemporal variability. On the inner shelf, BOD averaged $1.8 \pm 0.4 \text{ mmol N m}^{-2} \text{ d}^{-1}$ while mean N₂ production was $1.0 \pm 0.2 \text{ mmol N m}^{-2} \text{ d}^{-1}$. The difference between these values ($0.8 \pm 0.5 \text{ mmol N m}^{-2} \text{ d}^{-1}$) represents remineralized nitrogen that may be available to sustain regenerated production and is presumed to be the average efflux in spring and summer in section 3.5. In Table 3, published data over the entire shelf are provided for comparison. On the inner shelf, BOD was significantly higher than observed over the entire shelf ($p = 0.0001$) while mean N₂ was comparable to measurements over the entire shelf ($p = 0.69$).

3.5. Mass Balance Model for Nitrate and Ammonium

Using measurements of nutrient drawdown, assimilation, and efflux, a simple mass balance for nitrate and ammonium is used to provide estimates of the advection/diffusion of nutrients and ammonification in Region 7 of the inner shelf as follows:

$$d\text{NO}_3/dt = \text{Nitrification} - \text{Assimilation}_{(\text{NO}_3)} \pm \text{AdvDiff}_{(\text{NO}_3)} \quad (1)$$

$$d\text{NH}_4/dt = \text{Ammonification} + \text{Efflux} - \text{Nitrification} - \text{Assimilation}_{(\text{NH}_4)} \pm \text{AdvDiff}_{(\text{NH}_4)} \quad (2)$$

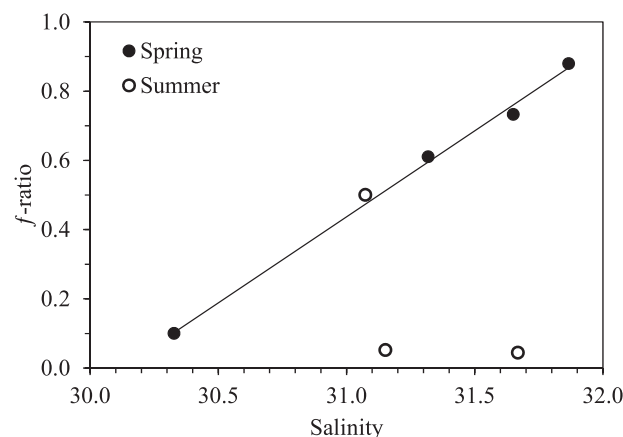


Figure 7. The relationship of the *f*-ratio with mean water column salinity. Stations were inshore of the 70 m isobath, and south of 60°N. The two stations on the middle shelf were in spring with $S > 31.6$, all other stations were on the inner shelf. In summer, values were low (high) in the absence (presence) of nutrient diffusion.

where *AdvDiff* is the advective-diffusive flux of nitrate or ammonium (negative values are net flux off the inner shelf). The model assumes that riverine inputs and the sediment flux of nitrate are negligible (discussed below). In equation (1), *AdvDiff*_(NO₃) is derived, and the ratio of NH₄/NO₃ on the middle shelf is used to convert this value into *AdvDiff*_(NH₄). Rates of nitrification on the inner shelf are estimated from integrated ammonium concentrations on the inner shelf each season, and the specific nitrification rate, λ_{nitrif} (the ammonium oxidation rate divided by the corresponding ammonium concentration) provided by Deal et al. [2008]. Parameters for spring and summer and the derived nutrient flux and

Table 3. Benthic Oxygen Demand (BOD) and N₂ Production Via Denitrification and/or Anammox at Stations on the Inner Shelf South of 60°N, and Summarized for All Shelf Data Collected During the Bering Sea Project

Cruise	Station	Date	Longitude (°W)	Latitude (°N)	Bottom Depth (m)	Benthic Oxygen Demand (mmol N m ⁻² d ⁻¹)	Denitrification/Anammox (mmol N m ⁻² d ⁻¹)
Inner Shelf							
HLY0902	9	7 Apr 2009	169.99	59.94	55	0.88 ± 0.05 (3)	0.86 ± 0.15 (2)
TN249	95	31 May 2010	163.28	57.64	46	2.4 (1)	
TN249	179	10 Jun 2010	168.16	58.83	46	2.8 ± 0.3 (2)	
TN250	39	24 Jun 2010	167.60	59.28	39	1.0 ± 0.2 (3)	0.8
TN250	83	1 Jul 2010	168.66	59.90	41	1.9 ± 0.3 (2)	1.3
Average inner shelf						1.8 ± 0.4 (5)	0.97 ± 0.15 (3)
Inner, middle and outer shelf						0.9 ± 0.1 (29) ^a	0.8 ± 0.1 (48) ^b

BOD was converted to nitrogen using an O₂:N ratio of 138:16. Denitrification/anammox was measured via mass balance at Station 9 and was directly measured as N₂ flux at Stations 39 and 83. Mean values are given as the mean ± SE (N). Note that in the Bering Sea Project, locations of stations and casts differ.

^aMean value determined from Table 2 in *Esch et al.* [2013].

^bMean value determined from Table 2 in *Horak et al.* [2013].

ammonification rates are shown in Table 4. Ammonification is specific to water column processes rather than sedimentary efflux. The results from this model suggest that nutrients are advected off the inner shelf in spring, but the reverse occurs in summer; and that ammonification is the greatest source of DIN on the inner shelf, especially in spring concomitant with ice-algal production and the spring phytoplankton bloom.

4. Discussion

During the earliest expedition (early April 2008), nitrate and ammonium concentrations in Region 7 were low, but not depleted, and similar to each other in magnitude (~3 μM, Figures 6a and 6b). These relatively high ammonium concentrations were consistent with remineralization of ice-algal production prior to our spring expedition. However, concurrent chlorophyll concentrations were extremely low (<1 μg L⁻¹, Figure 6c), suggesting that under-ice production was low, and measurements in 2008 might represent early-bloom conditions. In 2007, data were collected later in spring during ice retreat in that year (late April and early May), and concentrations more closely resemble spring bloom conditions with low nitrate and ammonium concentrations (<1 μM), and elevated chlorophyll concentrations (100–350 mg m⁻²). While the interannual patterns in Figures 6a and 6b are consistent with the seasonal drawdown of nutrients, this pattern could be the result of other processes (e.g., interannual variability in prebloom nutrient content, secondary production, or remineralization).

Table 4. Value of Parameters Used in the Mass Balance Model for Nitrate (Equation (1)) and Ammonium (Equation (2)) in Spring and Summer (±SD) for Region 7 of the Inner Shelf^a

Process	Units	Spring	Summer
Nutrient Drawdown			
dNO ₃ /dt	mmol m ⁻² d ⁻¹	-2.5 ± 0.5	0
dNH ₄ /dt	mmol m ⁻² d ⁻¹	-3.4 ± 0.7	0
Nitrification			
Specific nitrification rate	day ⁻¹	0.015	0.015
Integrated NH ₄	mmol m ⁻²	76 ± 58	10 ± 9
Nitrification rate	mmol m ⁻² d ⁻¹	1.1 ± 0.9	0.2 ± 0.1
Assimilation Rates			
NO ₃	mmol m ⁻² d ⁻¹	2.3 ± 2.7	0.5 ± 0.5
NH ₄	mmol m ⁻² d ⁻¹	8.7 ± 7.5	4.5 ± 4.4
Efflux (NH ₄)	mmol m ⁻² d ⁻¹	0.8 ± 0.5	0.8 ± 0.5
Advection/Diffusion			
[NH ₄]/[NO ₃] (middle shelf)		0.14 ± 0.13	0.45 ± 0.23
AdvDiff (NO ₃)	mmol m ⁻² d ⁻¹	-1.3 ± 2.8	0.3 ± 0.5
AdvDiff (NH ₄)	mmol m ⁻² d ⁻¹	-0.2 ± 0.4	0.1 ± 0.2
Ammonification	mmol m ⁻² d ⁻¹	5.8 ± 7.6	3.7 ± 4.4

^aThe specific nitrification rate is from *Deal et al.* [2008]; other values are from this study. Values in bold are derived from the model.

Nevertheless, rates of integrated nitrate and ammonium drawdown determined in section 3.2 were not significantly different from mean spring assimilation rates for each of these nutrients (Table 2, spring all years, $p = 0.7$ for nitrate $p = 0.06$ for ammonium), although other processes contribute to the nutrient mass balance (see equations (1) and (2)), and these are discussed below.

The timing and magnitude of chlorophyll accumulation in ice-covered waters in Region 7 (Figure 6c) were similar to the temporal variability observed in ice-free conditions on the inner shelf off Cape Newenham in April 1981 [*Whitledge et al.*, 1986,

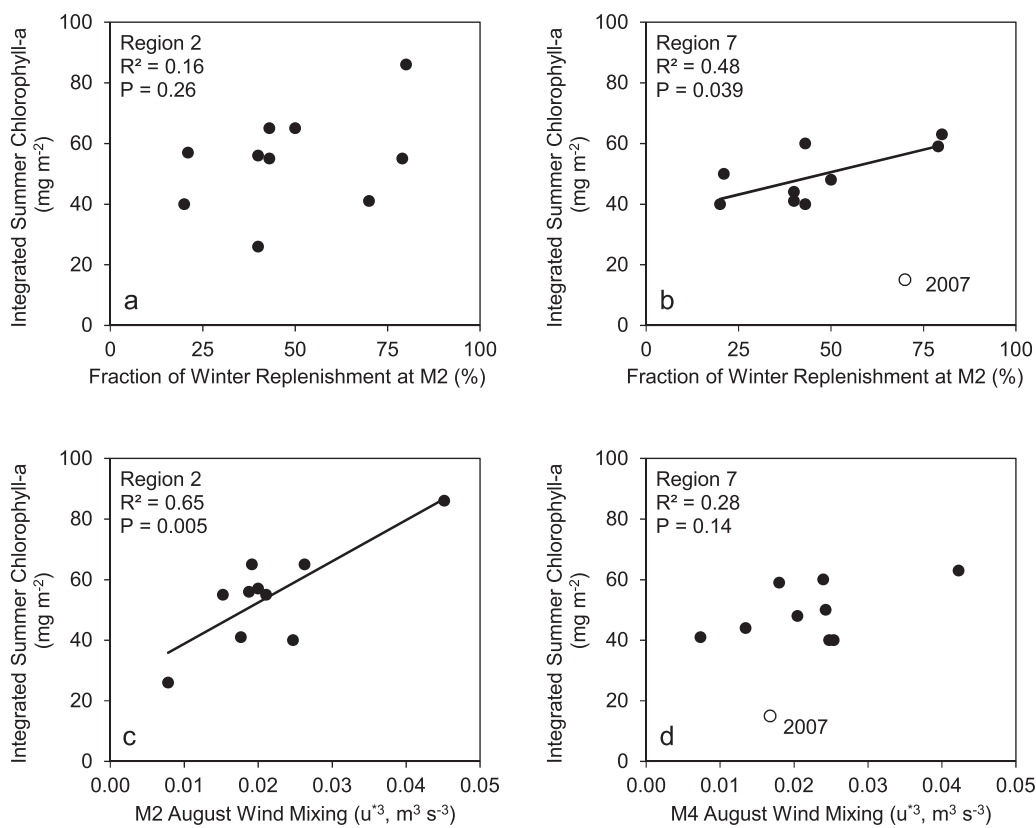


Figure 8. Relationships in (left) Region 2 and (right) Region 7 during late summer BASIS surveys of integrated chlorophyll *a* with (a, b) winter replenishment at M2, and August wind mixing at (c) M2 and (d) M4.

Figure 8] where they found that chlorophyll concentrations increased from ~ 50 to 100 mg m^{-2} during April. However, the nutrient content in *Whitledge et al.* [1986] was dramatically different than observed in this study. Along the 45 m isobath off Cape Newenham, April concentrations of nitrate ($\sim 8\text{--}12 \mu\text{M}$) and ammonium ($<1 \mu\text{M}$) favored new rather than regenerated production. Current speeds on the southern inner shelf are estimated at $\sim 2 \text{ cm s}^{-1}$, and imply that water sampled off Cape Newenham in April entered the shelf in early winter [Stabeno *et al.*, 2016]. Thus, this water had not been modified from a spring production cycle, and nitrate concentrations resembled fall concentrations in Bering Canyon ($5\text{--}22 \mu\text{M}$ nitrate between 30 and 40 m in a box from 54°N to 55°N , 165°W to 166.4°W in August–September, 2003–2014, $n = 44$, data from various NOAA programs). Conversely, during the ~ 1 year transit time to Region 7, these waters had been stripped of nutrients during the prior year's production cycle, and the nutrient content in April remained relatively low due to denitrification [Horak *et al.*, 2013] and weak flushing and nutrient replenishment in winter [Granger *et al.*, 2013]. Mass balance calculations suggest that in spring, water column ammonification is the greatest source of inorganic nitrogen on the shelf while the rate of nitrification is $\sim 50\%$ of nitrate assimilation. Hence, in Region 7, nutrients appear to be chronically low, and the system is largely regenerative even under the ice in spring (Figure 7).

During the Bering Sea Project, DIN concentrations on the middle shelf were significantly higher in spring 2008 compared to spring 2009, both in the north (stations between M5 and M8) and in the south (stations between M2 and M4) (Table 5) [Mordy *et al.*, 2012]. These data represent prebloom conditions and incorporate variability from replenishment and remineralization throughout the winter. Between M4 and M5, there was a consistent intrusion of fresher (<31.6) and nutrient-poor inner shelf water over the 70 m isobath each spring 2007–2009 [Mordy *et al.*, 2012]. Due to this feature, concentrations of DIN over the entire 70 m isobath were lower than DIN in the north or south (Table 5). This feature also implies concurrent replenishment over the inner shelf. The intensity of this feature varied among field years, and its signature salinity was preserved along the 70 m isobath in summer. Freshening was also observed in 2005 but was larger in extent and farther north, suggesting an ice-melt origin [Stabeno *et al.*, 2010].

Table 5. Comparison of Dissolved Inorganic Nitrogen (DIN) Concentrations in Early Spring 2008 and 2009 Along the 70 m Isobath^a

Region	DIN in 2008 (mmol N m ⁻²)	DIN in 2009 (mmol N m ⁻²)	p Value
North (M5–M8)	1079 ± 15 (20)	887 ± 18 (20)	<0.001
South (M2–M4)	1099 ± 21 (21)	1013 ± 33 (20)	0.033
All Stations (M2–M8)	975 ± 27 (58)	894 ± 22 (57)	0.023

^aRegions refer to portions of the 70 m isobath survey line between the designated moorings. Water column data were integrated to 70 m. Portions of this table were presented in *Mordy et al.* [2012].

Early spring freshening over the middle shelf, and implied replenishment on the inner shelf, was inconsistent with results of the mass balance model that was derived using all available spring data. The model showed a net loss of nutrients due to advection/diffusion (Table 4), although the propagated error of this result was quite large such that the net loss was not significantly different than zero (section 3.5). The

large error was primarily due to the variance between the three measurements of nitrate assimilation on the inner shelf. The lowest value in 2009 was most likely acquired during prebloom conditions while rates acquired during the spring bloom in 2007 were considerably higher (3.4 ± 2.6 SD mmol m⁻² d⁻¹, N = 2, supporting information Table S1). When substituting 2007 nitrate assimilation rates into equation (1), AdvDiff (NO₃) was approximately zero (-0.2 ± 2.8 SD mmol m⁻² d⁻¹). Similarly, there was uncertainty in dNO₃/dt in Table 4 due to the assumption that prebloom nutrient content on the inner shelf was similar in 2007, 2008, and 2009 (section 3.2), a faulty assumption if interannual differences observed on the middle shelf (Table 5) [*Mordy et al.*, 2012] extended to the inner shelf. If prebloom nitrate concentrations were similar in 2009 and 2007, a 30 day bloom results in dNO₃/dt of (-0.7 ± 0.6 SD mmol m⁻² d⁻¹) and a derived AdvDiff (NO₃) from equation (1) of (0.4 ± 2.9 SD mmol m⁻² d⁻¹). Hence, a combination of these refinements in the mass balance model can resolve these discrepancies between the mass balance model and observations of cross-shelf exchange. Despite these uncertainties, derived estimates of ammonification from equation (2) in spring were robust, and ranged from 5.4 to 5.8 mmol m⁻² d⁻¹ when applying these refinements. They support the notion that ammonification is greatest source of DIN on the inner shelf.

In summer, although nitrate was depleted on the inner shelf (<0.1 μM), there was measurable ammonium (0.33 ± 0.02 μM (144), Figure 6b). This implies that the moderate levels of chlorophyll biomass that were observed on the inner shelf (Figure 6c) were supported by regenerated production. This inference was verified by the very low *f*-ratios (0.05) observed at two summer stations on the inner front in 2010 (supporting information Table S1, Casts 18 and 46; Cast 117 is discussed below), and support other studies that hypothesize the inner shelf to be a net heterotrophic system [*Cross et al.*, 2014].

The sedimentary efflux of remineralized nitrogen appeared minor relative to assimilation rates. Assuming nearly all organic material reaching the benthos was oxidized [*Hartnett et al.*, 1998], BOD then reflects total ammonium regeneration. (This assumption is based upon oxygen penetration and bioturbation data on the Bering Sea shelf that are consistent with a long oxygen exposure time and a low burial efficiency on the shelf [*Esch et al.*, 2013].) A large fraction (53%) of regenerated ammonium was lost through denitrification/anammox (Table 3). The remaining fraction of remineralized nitrogen (0.8 ± 0.6 mmol N m⁻² d⁻¹) could efflux, but could only support ~15% of total nitrogen assimilation on the inner shelf (5.8 ± 5.5 mmol N m⁻² d⁻¹, Table 2).

While the efflux of remineralized nitrogen on the inner shelf was a minor fraction of primary production, efflux on the inner shelf appeared greater than in other shelf domains. BOD on the inner shelf was approximately twice as high as that for the entire eastern shelf, and there was no corresponding increase in N₂ production (Table 3). This implies that the efflux of remineralized organic nitrogen was significantly higher on the inner shelf compared to other domains. *Whitledge et al.* [1986] estimated a benthic release rate of 0.26 mmol N m⁻² d⁻¹ over the middle shelf in summer, and *Horak et al.* [2013] found that efflux of inorganic nitrogen was highly variable, but the shelf-wide average benthic flux in spring and summer was not significantly different from zero. Whereas the inner shelf exports more organic matter to the benthos [*Cross et al.*, 2014], the N₂ flux changes little, indicating that the rate of denitrification/anammox is not limited by the rate of sedimentary organic matter mineralization.

Other processes that may supply DIN to support summer production include the advective flux from Bristol Bay, riverine input, local ammonification/nitrification within the water column, and the advective/diffusive flux from the deep nutrient pool on the middle shelf. In summer, the alongshore advective DIN flux on the inner shelf was presumed to be small as the nutrient gradients from Bristol Bay to Nunivak were weak

[Kachel *et al.*, 2002; Whitedge *et al.*, 1986] and current speeds inshore of the inner front were low [Danielson *et al.*, 2011; Stabeno *et al.*, 2016]. Nor does there appear to be substantial input of nitrogen from the Kuskokwim River, the second largest river in Alaska. Sixty-three years of streamflow data are available from the USGS Crooked Creek monitoring station, which is located ~ 270 km upstream from the mouth of the river (National Water Information System, http://waterdata.usgs.gov/ak/nwis/inventory/?site_no=15304000). The mean discharge at Crooked Creek in summer (May–August) is $1.86 \times 10^8 \text{ m}^3 \text{ d}^{-1}$. When scaled to the size of the Kuskokwim watershed (1.54), the estimated discharge is $2.86 \times 10^8 \text{ m}^3 \text{ d}^{-1}$. Total nitrogen (DIN + organic nitrogen) was measured at five different sites along the river between 1975 and 1997 with a mean concentration of 39 ± 2 (90) μM (Water Quality Portal, <http://www.waterqualitydata.us/>). This equates to a discharge rate of $\sim 0.45 \text{ mmol N m}^{-2} \text{ d}^{-1}$ into Kuskokwim Bay (area of bay $\sim 25,000 \text{ km}^2$), which represents only a small fraction ($\sim 16\%$) of total nitrogen assimilation measured in Region 7 over the inner shelf in summer (Table 2). Danielson *et al.* [2011] found that, due to weak winds and frontal structures, most of this freshwater was retained inshore of the 30 m isobath during summer. However, Aguilar-Islas *et al.* [2007] observed significant concentrations of a terrestrial tracer (dissolved Mn) spreading out over the middle shelf. Thus, although riverine input may sporadically spread beyond the 30 m isobath and over the inner and middle shelves, it does not appear to contribute significantly to production on the inner shelf.

Within the water column, nitrification may serve as a significant source of DIN. For example, in 2005, there was evidence of nitrification within the water column as nitrite appeared to accumulate at the expense of ammonium [Mordy *et al.*, 2010], and Tanaka *et al.* [2004] found that nitrate in bottom waters of the middle shelf have a lighter isotopic signature that is consistent with nitrification. While specific rates of marine nitrification vary by several orders of magnitude [Yool *et al.*, 2007], results from a 1-D model in the Bering Sea suggest that $\lambda_{\text{nitrif}} = 0.015 \text{ day}^{-1}$ best replicates the seasonal dynamics observed for nitrate and ammonium [Deal *et al.*, 2008]. During the Bering Sea Project (2007–2010), integrated ammonium concentrations in Region 7 on the inner shelf (≤ 50 m water depth) were 76 ± 12 (24) mmol m^{-2} in spring, and 10 ± 2 (25) mmol m^{-2} in summer. From these concentrations and the specific rate provided by Deal *et al.* [2008], nitrification rates are estimated at 1.1 ± 0.2 and $0.3 \pm 0.1 \text{ mmol m}^{-2} \text{ d}^{-1}$ in spring and summer, respectively. These rates are about half of nitrate assimilation rates observed on the inner shelf (Tables 2 and 4), and support the conclusion of Granger *et al.* [2013] that much of the nitrate on the inner shelf is locally regenerated.

Diffusion at the inner front appears to sporadically inject nutrients onto the inner shelf. The location of the inner front undulates between shallower and deeper water depending upon winds and tides [Kachel *et al.*, 2002]. Hence, there are periods when the inner front abuts, diffuses, and erodes into the cooler nutrient-rich bottom layer of the middle shelf, and other periods when mixing is weaker and the inner front is shoreward of the deep nutrient pool. Along the MN Line in 2009, surface waters at the inner front were cooler with enhanced concentrations of silicic acid and a large accumulation of chlorophyll *a* (Figure 3). These features most likely originated from diffusion of the deep nutrient reservoir on the middle shelf, thereby enhancing primary production and resulting in the accumulation of chlorophyll *a*. While any diffusive flux of nitrate and ammonium appears to have been rapidly assimilated, enhanced concentrations of silicic acid likely reflect the absence of diatoms from the dominant phytoplankton species in summer [Moran *et al.*, 2012; Stoecker *et al.*, 2014]. In 2009, Cast 117 was centered in this cold band within the inner front (Figure 3). An *f*-ratio of 0.5 at this station was consistent with enhanced new production relative to other summer measurements (supporting information Table S1), and consistent with spring measurements at that salinity (Figure 7). Hence, residual silicic acid concentrations in summer may be used to identify potential regions and periods of new production despite the absence of nitrate. Correlation between weights of age-0 pollock (*Gadus chalcogrammus*) and summer silicic acid concentrations suggest that nondiatom productivity is a significant factor in the nourishment of pollock [Gann *et al.*, 2016]. An exception to this concept was observed north of the MN Line where silicic acid in surface waters were enhanced (Figure 5, section 3.1) despite stratification and a presumed reduction in vertical diffusion.

In 2009, the distinctive cold band associated with the inner front extended south to 57°N (Figure 5a). Yet there was little evidence of a diffusive nutrient flux south of the MN Line, as there was no surface expression of silicic acid (Figure 5c), nor shoaling of nutrient isolines or an accumulation of chlorophyll *a* on the NP Line (Figure 4). The location of the inner front (bar atop Figure 4) was determined using the definition in Kachel *et al.* [2002], and according to this definition, the front extended into the deep nutrient pool on the middle shelf. While coupled production of diatoms and grazers could have masked the diffusive flux

(drawdown of silicic acid and cropping of phytoplankton abundance), a more probable explanation is that the derivation of *Kachel et al.* [2002] exaggerated the seaward extent of the front into stratified waters where vertical mixing and the diffusive nutrient flux were greatly reduced. In their derivation, the offshore location of the front is relative to the intensity of the thermocline on the middle shelf (50% $|dT/dz|_{\max}$; see section 2.4). Along the NP Line in 2009, this placed the offshore location of the inner front at Cast 50; where the water depth was 56 m, the water column was stratified, and the temperature difference between surface and bottom waters was 4.6°C. A more plausible location for the seaward location of the inner front would be Cast 49, where the water depth was 46 m, the $|dT/dz|_{\max}$ was only 0.3°C, and the temperature difference between surface and deep water was only 0.5°C. This would place the inner front shoreward of the deep nutrient pool and account for the lack of chlorophyll and silicic acid in surface waters.

In other years, the diffusive flux was weak, but variable. In 2008, the deep pool of nitrate and silicic acid along the MN Line was farther offshore (~60 m isobath), temperatures at the inner front were warmer, and the concentration of chlorophyll *a* inshore of the 70 m isobath was $<2 \mu\text{g L}^{-1}$ (supporting information Figure S1). As the inner front was inshore of the 50 m isobath, the deep pool was too far offshore to be a source of nitrate and silicic acid at the front. However, the ammonium pool extended farther inshore and may have been available to support regenerated production. Along the NP Line, the inner front abutted the deep nutrient pool, resulting in a slight increase in silicic acid at the surface, and a small increase in chlorophyll *a* at the front (supporting information Figure S2). In 2010, due to late ice retreat and insufficient wind and tidal energy, there was a prominent low-salinity surface layer offshore of Nunivak Island that stratified the inner shelf and promoted warming of the upper water column. Hence, inner front had yet to develop along the MN Line (supporting information Figure S3). Although nitrate on the inner shelf was depleted, ammonium concentrations in the bottom layer were $\sim 2 \mu\text{M}$, and a subpycnocline chlorophyll *a* maximum extended inshore of the 50 m isobath (supporting information Figure S3).

Thus, the diffusive nutrient flux of DIN onto the inner shelf is an episodic event related to tidal and wind mixing but may be confounded by stratification over the inner shelf. This flux also depends on concentration in the deep nutrient pool of the middle shelf, which has significant seasonal and interannual variability (Table 5) [Mordy et al., 2012]. Variability in the deep nutrient pool may be ascribed to a variety of factors including winter replenishment [Stabeno et al., 2016], rates of primary production and remineralization [Lomas et al., 2012; Mordy et al., 2008, 2012], strength of stratification [Ladd and Stabeno, 2012], mixed layer depth [Stockwell et al., 2001], and erosion due to mixing and diffusion [Kachel et al., 2002].

Stabeno et al. [2016] estimated the fraction of water at the M2 mooring that was replenished by slope water each winter between 1995 and 2013. These estimates were based upon salinity changes at the mooring from the time the water column was well mixed (typically October) until February or the arrival of ice. While on average ~50% of water on the middle shelf is replenished each winter, there was extreme interannual variability with nearly complete (60–100%) replenishment in early 2000–2003, moderate replenishment in early 2008 (~40%), very little replenishment in early 2009 (~20%), and no detectable replenishment in spring 1997. These findings were consistent with higher DIN concentrations on the middle shelf in spring 2008 compared to 2009 (Table 2). Conditions in 1997 were exacerbated due to a strong May storm that mixed the water column at the M2 mooring to >50 m [Stockwell et al., 2001]. Calm conditions followed, resulting in a relatively shallow (10–15 m) mixed layer and a subpycnocline euphotic zone. By June, subpycnocline production had consumed all but 4 μM nitrate in the bottom 20 m of the water column on the middle shelf [Stockwell et al., 2001]. Hence, the diffusive nutrient flux and postbloom production at the inner front are presumed to have been anomalously low in 1997.

Interannual variability in the late-summer time series of integrated chlorophyll in Regions 2 and 7 might be attributed in part to the diffusive flux of DIN along the inner front. In August, integrated chlorophyll *a* concentrations in Region 2, the region adjacent to the M2 mooring, were not significantly correlated with winter replenishment (Figure 8a). This result was not too surprising as waters at M2 would have advected $\sim 2^\circ$ north in the six months between estimates of winter replenishment at M2 (February) and BASIS measurements of chlorophyll *a* (August) [Stabeno et al., 2016]. Farther north, in Region 7, there was a significant relationship between winter replenishment estimates made at M2 and integrated chlorophyll *a* on the inner shelf (Figure 8b, excluding 2007, which is discussed below). This finding supports the hypothesis that interannual variability in the nutrient pool at the onset of spring modifies the nutrient flux across the inner front farther north in summer.

In Region 2, integrated chlorophyll *a* during BASIS was significantly related to wind mixing (Figure 8c). Similar relationships were observed on the middle shelf between wind mixing and net community production [Mordy *et al.*, 2012], and between wind mixing and integrated chlorophyll *a* [Eisner *et al.*, 2016]; and these relationships were attributed to vertical mixing of the deep nutrient pool. On the inner shelf, stratification was generally weak and DIN concentrations in the water column during BASIS were low (average DIN = 0.7 μM , except for 2007 when DIN averaged 2.1 μM). Increased winds likely expanded the inner front seaward and enhanced erosion of the nutrient pool on the middle shelf. However, this relationship did not hold for Region 7 (Figure 8d), demonstrating that factors other than winds and undulation of the inner front (e.g., grazing) were controlling chlorophyll *a* concentrations.

Chlorophyll *a* was anomalously low in 2007, both on the middle and inner shelves (Figures 8b and 8d) [Eisner *et al.*, 2016]. In most years, waters over the inner shelf were well mixed in summer. In 2010, ice retreat was late and forestalled mixing on parts of the inner shelf (supporting information Figure S3), but by late August 2010, the water column in Region 7 was well mixed with a mean dT/dz_{max} of 0.2°C. In 2007, the timing of ice retreat was not unusual; however, there were very few storms [Eisner *et al.*, 2016], and moderate winds in August were insufficient to mix the water column. As a result, the water column just south of Nunivak Island remained stratified in late August with an intense thermocline (mean dT/dz_{max} = 9.0°C). This band of stratified water disrupted the inner front in Region 7 and likely reduced the flux of nutrients that are normally supplied through wind and tidal mixing.

5. Summary

In the vicinity of Nunivak Island, waters over the inner shelf are modified during the ~ 1 year transit from Bering Canyon, including the drawdown of nitrate from the previous year's production cycle. In spring, due to limited flushing in fall/winter and additional nitrogen loss through denitrification/anammox, initial nitrate concentrations on the inner shelf near Nunivak Island remain relatively low and comparable to ammonium. As a result, production over the inner shelf is regenerative, even in spring. As the system progresses from a diatom system in spring to a microflagellate system in summer, there remains little inorganic nitrogen on this portion of the inner shelf. Relative to rates of primary production, sedimentary regeneration and efflux of DIN are low, as is the supply of dissolved and organic N supply from the Kuskokwim River, and the advective nutrient flux from Bristol Bay. Therefore, most of the inorganic nitrogen supply on the inner shelf is provided through resuspended sediments, water column remineralization, and the diffusive flux at the inner front. The episodic diffusive flux of nutrients at the inner front promotes new production and may be identified from residual silicic acid at the surface. Gann *et al.* [2016] identified a relationship between residual silicic acid and age-0 pollock (length and weight), suggesting a link between nutrient supply, phytoplankton growth, and energy transfer to higher trophic levels.

Hence, the inner shelf in Region 7 appears to be regenerative in all seasons, except where diffusion injects new nitrogen at the inner front (or stratification extends over the inner shelf as in 2010). The diffusive flux is dependent in part on stratification, wind mixing, and winter replenishment of bottom waters on the middle shelf. Correlations between winter replenishment and summertime concentrations of phytoplankton biomass (i.e., chlorophyll *a*) over portions of the inner shelf indicate that the influence of winter replenishment on the ecosystem is prolonged, and partly governs energy flow through the ecosystem. The new findings in this study include the availability and drawdown of spring nutrients in ice-covered waters of the inner shelf, direct measurements on the regenerative nature of the inner shelf, especially in spring, and the spatiotemporal variability of the diffusive nutrient flux, and its connectivity to winter replenishment. Additional sampling and time series measurements on the inner shelf will help to refine our understanding of the nitrogen cycle, and reduce uncertainties in the advective-diffusive flux of nitrate and ammonium, and rates of ammonification on the inner shelf.

References

- Aguilar-Islas, A. M., M. P. Hurst, K. N. Buck, B. Sohst, G. J. Smith, M. C. Lohan, and K. W. Bruland (2007), Micro- and macronutrients in the southeastern Bering Sea: Insight into iron-replete and iron-depleted regimes, *Prog. Oceanogr.*, 73(2), 99–126.
- Chang, B. X., and A. H. Devol (2009), Seasonal and spatial patterns of sedimentary denitrification rates in the Chukchi Sea, *Deep Sea Res., Part II*, 56(17), 1339–1350, doi:10.1016/j.dsr2.2008.10.024.
- Coachman, L. K. (1986), Circulation, water masses, and fluxes on the southeastern Bering Sea shelf, *Cont. Shelf Res.*, 5(1), 23–108.

Acknowledgments

We thank the many officers and crew members from each of the research surveys for their assistance and effort. We also thank the staff and research technicians at each of the contributing laboratories, especially Shaun Bell and Peggy Sullivan for data management, Sigrid Salo for compiling and analyzing satellite data, and Karen Birchfield for assisting with the figures. Thanks to George Hunt and an anonymous reviewer for very constructive comments. Data supporting the conclusions can be obtained from the BEST-BSIERP Data Archive (<http://beringsea.eol.ucar.edu/>). Research was funded by NSF grants ARC-0732430 and ARC-0732640 (C.W. Mordy), ARC-0732359 (M.W. Lomas), ARC-0612380 and MRI-0723234 (D.H. Shull), ARC-0623174 (A. Devol), and ARC-0612427 (R. Sambrotto). This publication was partially funded by the Joint Institute for the Study of the Atmosphere and Ocean (JISAO) under NOAA Cooperative Agreements NA17RJ1232 and NA10OAR4320148 and is contribution 0872 to NOAA's Ecosystems and Fisheries-Oceanography Coordinated Investigations, contribution 2716 to JISAO, and contribution 4494 to NOAA's Pacific Marine Environmental Laboratory.

- Coyle, K. O., and A. I. Pinchuk (2002), Climate-related differences in zooplankton density and growth on the inner shelf of the southeastern Bering Sea, *Prog. Oceanogr.*, *55*(1), 177–194, doi:10.1016/S0079-6611(02)00077-0.
- Coyle, K. O., L. B. Eisner, F. J. Mueter, A. I. Pinchuk, M. A. Janout, K. D. Cieciel, E. V. Farley, and A. G. Andrews (2011), Climate change in the southeastern Bering Sea: Impacts on pollock stocks and implications for the oscillating control hypothesis, *Fish. Oceanogr.*, *20*(2), 139–156, doi:10.1111/j.1365-2419.2011.00574.x.
- Cross, J. N., et al. (2014), Integrated assessment of the carbon budget in the Southeastern Bering Sea, *Deep Sea Res., Part II*, *109*, 112–124, doi:10.1016/j.dsr2.2014.03.003.
- Danielson, S., L. Eisner, T. Weingartner, and K. Aagaard (2011), Thermal and haline variability over the central Bering Sea shelf: Seasonal and interannual perspectives, *Cont. Shelf Res.*, *31*(6), 539–554, doi:10.1016/j.csr.2010.12.010.
- Davenport, E. S., D. H. Shull, and A. H. Devol (2012), Roles of sorption and tube-dwelling benthos in the cycling of phosphorus in Bering Sea sediments, *Deep Sea Res., Part II*, *65*, 163–172, doi:10.1016/j.dsr2.2012.02.004.
- Deal, C. J., J. Meibing, and W. Jia (2008), The significance of water column nitrification in the southeastern Bering Sea, *Chin. J. Polar Sci.*, *19*(2), 185–192.
- Dugdale, R. C., and J. J. Goering (1967), Uptake of new and regenerated forms of nitrogen in primary productivity, *Limnol. Oceanogr.*, *12*(2), 196–206.
- Eisner, L. B., J. C. Gann, C. Ladd, K. D. Cieciel, and C. W. Mordy (2016), Late summer/early fall phytoplankton biomass (chlorophyll *a*) in the eastern Bering Sea: Spatial and temporal variations and factors affecting chlorophyll-*a* concentrations, *Deep Sea Res., Part II*, *134*, 100–114, doi:10.1016/j.dsr2.2015.07.012.
- Esch, M. E. S., D. H. Shull, and A. H. Devol (2013), Regional patterns of bioturbation and iron and manganese reduction in the sediments of the southeastern Bering Sea, *Deep Sea Res., Part II*, *94*, 80–94.
- Gann, J. C., et al. (2016), Possible mechanism linking ocean conditions to low body weight and poor recruitment of age-0 walleye pollock (*Gadus chalcogrammus*) in the southeast Bering Sea during 2007, *Deep Sea Res., Part II*, *134*, 115–137, doi:10.1016/j.dsr2.2015.07.010.
- Gordon, L. I., J. C. Jennings Jr., A. A. Ross, and J. M. Krest (1993), A suggested protocol for continuous flow automated analysis of seawater nutrients (phosphate, nitrate, nitrite and silicic acid) in the WOCE Hydrographic Program and the Joint Global Ocean Fluxes Study, in *Methods Manual WHPO 91-1*, WHP Oper. and Methods, WOCE Hydrogr. Program Off., La Jolla, Calif.
- Granger, J., M. G. Prokopenko, C. W. Mordy, and D. M. Sigman (2013), The proportion of remineralized nitrate on the ice-covered eastern Bering Sea shelf evidenced from the oxygen isotope ratio of nitrate, *Global Biogeochem. Cycles*, *27*, 962–971, doi:10.1002/gbc.20075.
- Hartnett, H. E., R. G. Keil, J. I. Hedges, and A. H. Devol (1998), Influence of oxygen exposure time on organic carbon preservation in continental margin sediments, *Nature*, *391*, 572–575.
- Horak, R. E. A., H. Whitney, D. H. Shull, C. W. Mordy, and A. H. Devol (2013), The role of sediments on the Bering Sea shelf N cycle: Insights from measurements of benthic denitrification and benthic DIN fluxes, *Deep Sea Res., Part II*, *94*, 95–105, doi:10.1016/j.dsr2.2013.03.014.
- Kachel, N. B., G. L. Hunt Jr., S. A. Salo, J. D. Schumacher, P. J. Stabeno, and T. E. Whitledge (2002), Characteristics and variability of the inner front of the southeastern Bering Sea, *Deep Sea Res., Part II*, *49*(26), 5889–5909, doi:10.1016/S0967-0645(02)00324-7.
- Kalnay, E., et al. (1996), The NCEP/NCAR 40-year reanalysis project, *Bull. Am. Meteorol. Soc.*, *77*, 437–470.
- Kana, T. M., C. Darkangelo, M. D. Hunt, J. B. Oldham, G. E. Bennett, and J. C. Cornwell (1994), Membrane inlet mass spectrometer for rapid high-precision determination of N₂, O₂, and Ar in environmental water samples, *Anal. Chem.*, *66*(23), 4166–4170, doi:10.1021/ac00095a009.
- Kanamitsu, M., W. Ebisuzaki, J. Woollen, S.-K. Yang, J. J. Hnilo, M. Fiorino, and G. L. Potter (2002), NCEP-DOE AMIP-II Reanalysis (R-2), *Bull. Am. Meteorol. Soc.*, *83*, 1631–1643.
- Kinder, T. H., and J. D. Schumacher (1981a), Hydrographic structure over the continental shelf of the southeastern Bering Sea, in *The Eastern Bering Sea Shelf: Oceanography and Resources*, vol.1, edited by D. W. Hood and J. A. Calder, pp. 31–52, NOAA Off. of Mar. Pollut. Assess., distributed by the Univ. of Wash. Press, Seattle.
- Kinder, T. H., and J. D. Schumacher (1981b), Circulation over the continental shelf of the southeastern Bering Sea, in *The Eastern Bering Sea Shelf: Oceanography and Resources*, vol.1, edited by D. W. Hood and J. A. Calder, pp. 53–75, NOAA Off. of Mar. Pollut. Assess., distributed by the Univ. of Wash. Press, Seattle.
- Ladd, C., and N. A. Bond (2002), Evaluation of the NCEP/NCAR reanalysis in the NE Pacific and the Bering Sea, *J. Geophys. Res.*, *107*(C10), 3158, doi:10.1029/2001JC001157.
- Ladd, C., P. J. Stabeno, and J. E. O'Hern (2012), Observations of a Pribilof eddy, *Deep Sea Res., Part I*, *66*, 67–76, doi:10.1016/j.dsr.2012.04.003.
- Lomas, M. W., S. B. Moran, J. R. Casey, D. W. Bell, M. Tiahlo, J. Whitefield, R. P. Kelly, J. T. Mathis, and E. D. Cokelet (2012), Spatial and seasonal variability of primary production on the eastern Bering Sea shelf, *Deep Sea Res., Part II*, *65–70*, 126–140, doi:10.1016/j.dsr2.2012.02.010.
- Mantoura, R. F. C., and E. M. S. Woodward (1983), Optimization of the indophenol blue method for the automated determination of ammonia in estuarine waters, *Estuarine Coastal Shelf Sci.*, *17*(2), 219–224.
- Moran, S. B., M. W. Lomas, R. P. Kelly, R. Gradinger, K. Iken, and J. T. Mathis (2012), Seasonal succession of net primary productivity, particulate organic carbon export, and autotrophic community composition in the eastern Bering Sea, *Deep Sea Res., Part II*, *65*, 84–97, doi:10.1016/j.dsr2.2012.02.011.
- Mordy, C. W., P. J. Stabeno, D. Righi, and F. A. Menzia (2008), Origins of the subsurface ammonium maximum in the southeast Bering Sea, *Deep Sea Res., Part II*, *55*(16), 1738–1744, doi:10.1016/j.dsr2.2008.03.005.
- Mordy, C. W., L. B. Eisner, P. Proctor, P. Stabeno, A. H. Devol, D. H. Shull, J. M. Napp, and T. Whitledge (2010), Temporary uncoupling of the marine nitrogen cycle: Accumulation of nitrite on the Bering Sea shelf, *Mar. Chem.*, *121*(1), 157–166.
- Mordy, C. W., E. D. Cokelet, C. Ladd, F. A. Menzia, P. Proctor, P. J. Stabeno, and E. Wisegarver (2012), Net community production on the middle shelf of the Eastern Bering Sea, *Deep Sea Res., Part II*, *65–70*, 110–125, doi:10.1016/j.dsr2.2012.02.012.
- Ortiz, I., F. Weise, and A. Greig (2012), *Marine Regions Boundary Data for the Bering Sea Shelf and Slope*, UCAR/NCAR—Earth Obs. Lab., Boulder, Colo., doi:10.5065/D6DF6P6C. [Available at <http://data.eol.ucar.edu/codiac/dss/id=245.B99-001>.]
- Overland, J. E., S. A. Salo, L. H. Kantha, and C. A. Clayson (1999), Thermal stratification and mixing on the Bering Sea shelf, in *Dynamics of the Bering Sea*, edited by T. R. Loughlin and K. Ohtani, pp. 129–146, Alaska Sea Grant Coll. Program, Fairbanks.
- Redfield, A. C. (1958), The biological control of chemical factors in the environment, *Am. Sci.*, *46*, 205–221.
- Rho, T., and T. E. Whitledge (2007), Characteristics of seasonal and spatial variations of primary production over the southeastern Bering Sea shelf, *Cont. Shelf Res.*, *27*, 2556–2569.
- Sambrotto, R. N., H. J. Niebauer, J. J. Goering, and R. L. Iverson (1986), Relationships among vertical mixing, nitrate uptake, and phytoplankton growth during the spring bloom in the southeast Bering Sea middle shelf, *Cont. Shelf Res.*, *5*(1), 161–198.

- Sambrotto, R. N., D. Burdloff, and K. McKee (2016), Spatial and year-to-year patterns in new and primary productivity in sea ice melt regions of the eastern Bering Sea, *Deep Sea Res., Part II*, 134, 86–99, doi:10.1016/j.dsr2.2015.07.011.
- Schumacher, J. D., and P. J. Stabeno (1998), The continental shelf of the Bering Sea, in *The Sea*, vol. 11, edited by A. R. Robinson and K. H. Brink, pp. 789–822, John Wiley, New York.
- Schumacher, J. D., T. H. Kinder, D. J. Pashinski, and R. L. Charnell (1979), A structural front over the continental shelf of the eastern Bering Sea, *J. Phys. Oceanogr.*, 9(1), 79–87, doi:10.1175/1520-0485(1979)009<0079:ASFOTC>2.
- Sigler, M. F., P. J. Stabeno, L. B. Eisner, J. M. Napp, and F. J. Mueter (2014), Spring and fall phytoplankton blooms in a productive subarctic ecosystem, the eastern Bering Sea, during 1995–2011, *Deep Sea Res., Part II*, 109, 71–83, doi:10.1016/j.dsr2.2013.12.007.
- Stabeno, P. J., J. D. Schumacher, and K. Ohtani (1999), The physical oceanography of the Bering Sea, in *Dynamics of the Bering Sea: A Summary of Physical, Chemical, and Biological Characteristics, and a Synopsis of Research on the Bering Sea*, edited by T. R. Loughlin and K. Ohtani, pp. 1–28, Univ. of Alaska Sea Grant, North Pac. Mar. Sci. Org., Fairbanks, Alaska.
- Stabeno, P. J., N. A. Bond, N. B. Kachel, S. A. Salo, and J. D. Schumacher (2001), On the temporal variability of the physical environment over the south-eastern Bering Sea, *Fish. Oceanogr.*, 10(1), 81–98.
- Stabeno, P. J., N. Kachel, C. Mordy, D. Righi, and S. Salo (2008), An examination of the physical variability around the Pribilof Islands in 2004, *Deep Sea Res., Part II*, 55(16–17), 1701–1716, doi:10.1016/j.dsr2.2008.03.006.
- Stabeno, P. J., J. Napp, C. Mordy, and T. Whitedge (2010), Factors influencing physical structure and lower trophic levels of the eastern Bering Sea shelf in 2005: Sea ice, tides and winds, *Prog. Oceanogr.*, 85(3–4), 180–196, doi:10.1016/j.pocan.2010.02.010.
- Stabeno, P. J., E. V. Farley Jr., N. B. Kachel, S. Moore, C. W. Mordy, J. M. Napp, J. E. Overland, A. I. Pinchuk, and M. F. Sigler (2012a), A comparison of the physics of the northern and southern shelves of the eastern Bering Sea and some implications for the ecosystem, *Deep Sea Res., Part II*, 65–70, 14–30, doi:10.1016/j.dsr2.2012.02.019.
- Stabeno, P. J., N. B. Kachel, S. E. Moore, J. M. Napp, M. Sigler, A. Yamaguchi, and A. N. Zerbini (2012b), Comparison of warm and cold years on the southeastern Bering Sea shelf and some implications for the ecosystem, *Deep Sea Res., Part II*, 65–70, 31–45, doi:10.1016/j.dsr2.2012.02.020.
- Stabeno, P. J., S. Danielson, D. Kachel, N. B. Kachel, and C. W. Mordy (2016), Currents and transport on the eastern Bering Sea shelf: An integration of over 20 years of data, *Deep Sea Res., Part II*, 134, 13–29, doi:10.1016/j.dsr2.2016.05.010.
- Stockwell, D. A., T. E. Whitedge, S. I. Zeeman, K. O. Coyle, J. M. Napp, R. D. Brodeur, A. I. Pinchuk, and G. L. Hunt (2001), Anomalous conditions in the south-eastern Bering Sea, 1997: Nutrients, phytoplankton and zooplankton, *Fish. Oceanogr.*, 10(1), 99–116.
- Stoecker, D. K., A. C. Weigel, D. A. Stockwell, and M. W. Lomas (2014), Microzooplankton: Abundance, biomass and contribution to chlorophyll in the Eastern Bering Sea in summer, *Deep Sea Res., Part II*, 109, 134–144, doi:10.1016/j.dsr2.2013.09.007.
- Strickland, J. D. H., and T. R. Parsons (1972), *A Practical Handbook of Seawater Analysis*, 2nd ed., Bull. 167, Fish. Res. Board of Canada, Ottawa, Canada.
- Sullivan, M. E., N. B. Kachel, C. W. Mordy, and P. J. Stabeno (2008), The Pribilof Islands: Temperature, salinity and nitrate during summer 2004, *Deep Sea Res., Part II*, 55(16), 1729–1737, doi:10.1016/j.dsr2.2008.03.004.
- Tanaka, T., L. Guo, C. Deal, N. Tanaka, T. Whitedge, and A. Murata (2004), N deficiency in a well-oxygenated cold bottom water over the Bering Sea shelf: Influence of sedimentary denitrification, *Cont. Shelf Res.*, 24(12), 1271–1283.
- Whitedge, T. E., W. S. Reeburgh, and J. J. Walsh (1986), Seasonal inorganic nitrogen distributions and dynamics in the southeastern Bering Sea, *Cont. Shelf Res.*, 5(1), 109–132.
- Yool, A., A. P. Martin, C. Fernández, and D. R. Clark (2007), The significance of nitrification for oceanic new production, *Nature*, 447(7147), 999–1002, doi:10.1038/nature05885.
- Zador, S. (Ed.) (2013), *Ecosystem Considerations for 2013*, Plan Teams for the Groundfish Fish. of the Bering Sea, Aleutian Isl., and Gulf of Alaska, North Pac. Fish. Manage. Council, Anchorage.